Organic Electronics 32 (2016) 89–93

Contents lists available at ScienceDirect

Organic Electronics

journal homepage: www.elsevier.com/locate/orgel

Letter

Improved quantum dot light-emitting diodes with a cathode interfacial layer

Tao Ding [a], Xuyong Yang [a], Lin Ke [c], Yanjun Liu [c], Wan-Yi Tan [d], Ning Wang [a], Xu-Hui Zhu [d, **], Xiao Wei Sun [a, b, *]

[a] *LUMINOUS! Centre of Excellence for Semiconductor Lighting and Displays, School of Electrical and Electronic Engineering, Nanyang Technological University, 50 Nanyang Avenue, 639798, Singapore*
[b] *Department of Electrical and Electronic Engineering, College of Engineering, South University of Science and Technology of China, 1088 Xueyuan Road, Nanshan, Shenzhen 518055, China*
[c] *Institute of Materials Research and Engineering, A*STAR (Agency for Science, Technology and Research), 3 Research Link, 117602, Singapore*
[d] *State Key Laboratory of Luminescent Materials and Devices (SKLLMD), Institute of Polymer Optoelectronic Materials and Devices, South China University of Technology, Guangzhou 510640, China*

ARTICLE INFO

Article history:
Received 30 December 2015
Received in revised form
21 January 2016
Accepted 14 February 2016
Available online xxx

Keywords:
Quantum dot
Light-emitting diodes
Cathode interfacial material
Electron/hole-only devices
Charge balance

ABSTRACT

Colloidal quantum dot light-emitting diodes (QLEDs) are reported with improved external quantum efficiencies (EQE) and efficiency roll-off under high current densities by introducing a thermally-evaporated organic cathode interfacial material (CIM) Phen-NaDPO. QLEDs with this new CIM modified Al cathode were fabricated, giving an upwards of 25% enhancement in the EQE relative to the bare Al device. Ultraviolet photoemission spectroscopy (UPS) suggests that this material can effectively lower the work function of Al, therefore facilitating the electron injection in QLEDs. Furthermore, Phen-NaDPO was introduced into the LiF/Al device to afford better balanced hole/electron injection in the emitting layer. Consequently, the QLEDs with the organic CIM/LiF/Al cathode further increased EQE and current efficiency by 44% and 52%, respectively, with higher luminance and lower efficiency roll-off under high current densities.

1. Introduction

Since their first appearance for more than two decades [1,2], quantum dot light-emitting diodes (QLEDs) have emerged as a qualified candidate for the next-generation solid-state lighting and display technologies due to their tunable wavelength covering the whole visible range, narrow full-width at half-maximum (FWHM) and excellent color saturation features [3–10]. Recent reports have demonstrated that QLEDs can achieve comparable levels of efficiency with better color saturation and lower cost compared with organic LEDs (OLEDs) [4,6]. For most of the reported high-efficient QLEDs, the combination of spin-coating and thermal evaporation techniques is frequently employed for device fabrication. A challenge for solution process is that orthogonal solvents are required to avoid interlayer mixing [4,7,8,11].

Lithium fluoride (LiF) is frequently used as the cathode interfacial material to improve the electron injection by reducing the work function of the cathode (aluminum in the most cases) in QLED fabrication [12–15], which has been explained by the reduced injection barrier resulting from the band bending [16], the tunneling theory [32] and the decreased surface potential of cathode resulted from the large dipole moment of LiF [33]. However, the insulating property of the inorganic LiF could result in high processing temperature (over 600 °C) during thermal evaporation process and difficult control of the thickness of the thin film (generally less than 1 nm) [17]. The high evaporating temperature might deteriorate the underlying organic active layers, harming device performance [18]. Besides LiF, other inorganic cathode modification materials, including cesium carbonate [19], cesium fluoride [20] and low work-function metals including magnesium [21–23] and calcium [24,25] have been reported in order to reduce the injection barriers and improve the device performance.

Here, we introduce an efficient organic cathode interfacial material (CIM) called 1,10-phenanthroline-(2-naphthyl)diphenylphosphine oxide (Phen-NaDPO) for improving the device

* Corresponding author. LUMINOUS! Centre of Excellence for Semiconductor Lighting and Displays, School of Electrical and Electronic Engineering, Nanyang Technological University, 50 Nanyang Avenue, 639798, Singapore
** Corresponding author.
E-mail addresses: xuhuizhu@scut.edu.cn (X.-H. Zhu), sunxw@sustc.edu.cn (X.W. Sun).

http://dx.doi.org/10.1016/j.orgel.2016.02.018
1566-1199/

performance. Phen-NaDPO possesses an electron mobility of 3.9×10^{-4} cm^2 V^{-1} s^{-1} (at E = ~8×10^5 V cm^{-1}) and a glass transition temperature (T_g) of 116 °C, and has been successfully demonstrated as a versatile CIM by improving the power conversion efficiency (PCE) in organic photovoltaics [26]. In our QLEDs, introducing this material between the electron transporting layer and the cathode produced better device performance including external quantum efficiency (EQE), current efficiency (CE) and power efficiency (PE) when compared with those of pristine Al-based device. Further, in contrast with the LiF-based devices, both CE and PE are improved while the maximum luminance is comparable. An even higher EQE of 8.5% is achieved by incorporating Phen-NaDPO with LiF/Al as the cathode, vs. 7.4% of the Phen-NaDPO/Al cathode, with smaller efficiency roll-off under high current densities. UPS measurements combined with the analysis of the current density-voltage characteristics of the single-carrier devices are utilized to explain our results.

2. Experimental details

2.1. Materials

Synthesis of quantum dots: The CdSe@ZnS core-shell quantum dots (QDs) were synthesized according to the previously reported procedure with some modifications [5]. Briefly, 0.14 mmol of cadmium acetate, 3.41 mmol of zinc oxide and 7 ml of oleic acid (OA) were mixed in a four-neck flask and heated to 100 °C with degassing under 0.03 mTorr pressure for 20 min. Then, 15 ml of 1-octadecene (1-ODE) was added into the reactor, and the whole mixture was degassed again and heated up to 100 °C. The reactor was filled with Argon and further heated to 310 °C. Then, 2 mmol of selenium (Se) and 2 mmol of sulfur (S) dissolved in 2 ml tri-octylphosphine (TOP) was swiftly injected into the hot mixture, followed by holding the reaction for 10 min. In order to coat an additional ZnS shell, 1.6 mmol of S with 2.4 ml of ODE was injected and the mixture was left to react for 12 min. Then 9.5 ml $Zn(OA)_2$ was injected and the temperature was controlled to 270 °C. Next, 5 ml of TOP containing 9.65 mmol of S was injected into the mixture at a rate of 10 ml/min. The resulting reaction was maintained at that temperature for 20 min. The QDs were further purified and re-dispersed in toluene for later use in QLEDs.

2.1.1. Device fabrication and characterization

ITO detergent, de-ionized water, acetone and isopropyl alcohol were used to sequentially clean the glass substrates with patterned ITO. A layer of poly (3,4-ethylenedioxythiophene)-poly(styrenesulfonate) (PEDOT:PSS)was spin-coated at 4000 rpm and baked for 30 min, followed by 30 nm of poly(9-vinylcarbazole) (PVK) serving as hole transport layer. The QD layer was deposited on the ITO/PEDOT:PSS/PVK at a speed of 1000 rpm for 60s and subsequently annealed at 90 °C for 30 min. Then, on top of the QD layer, 2,2′,2″ - (1,3,5-Benzinetriyl) - tris(1-phenyl-1-H-benzimidazole) (TPBi), CIM and Al were sequentially thermal-evaporated under a base pressure of ~1.0×10^{-6} Pa. The effective area of the LED devices is 4 mm^2.

UPS measurement was performed by using X-Ray Photoelectron Spectroscopy (XPS) (VG Escalab 220i XL) with a He I (21.2 eV) gas discharge lamp. The current density-luminance-voltage (J-L-V) characteristics were measured using a programmable Yogakawa GS610 source measurement unit. The electroluminescence spectra of the QD-LEDs were acquired by a PhotoResearch SpectraScan PR 705 spectrometer. All measurements were carried out at room temperature under ambient atmosphere without any encapsulation.

3. Results and discussion

Fig. 1(a) shows the normalized electroluminescence (EL) spectrum with an emission peak wavelength at 522 nm and a full width at half maximum (FWHM) of 20 nm. The device structure of the QLED discussed here is depicted in Fig. 1(b), where the CIM layer is inserted between the Al cathode and TPBi (the electron transport layer) to facilitate electron injection. Phen-NaDPO was thermally evaporated before cathode deposition. Fig. 2(a) shows the current density-voltage-luminance (*J-V-L*) characteristics of the QLEDs involving Al-only and Phen-NaDPO (with different thicknesses)/Al cathodes. It can be clearly seen that the devices with Phen-NaDPO-modified cathode show better performance than the Al-only devices, yielding a maximum brightness over 100,000 cd/m^2 with a 9 nm-thickness CIM. The EQE and current efficiency (CE) as a function of current density for these QLEDs are shown in Fig. 2(b). A peak EQE of 7.4% and maximum CE of 24 cd/A are achieved with the optimized QLED. In contrast, the device with pristine Al as the cathode demonstrates inferior performance with a maximum EQE lower than 6% and a lower peak brightness, as can be seen by Fig. 2(a) and (b).

Next, the performance of the optimized Phen-NaDPO-based device is compared to the LiF/Al-cathode based QLED. As can been seen from Fig. 3 (a), the Phen-NaDPO-based QLED shows comparable *J-V-L* characteristics with those of the LiF-based device. On the other hand, higher EQE (7.4%) and CE (24.1 cd/A) have been achieved by Phen-NaDPO device compared with LiF-based QLED

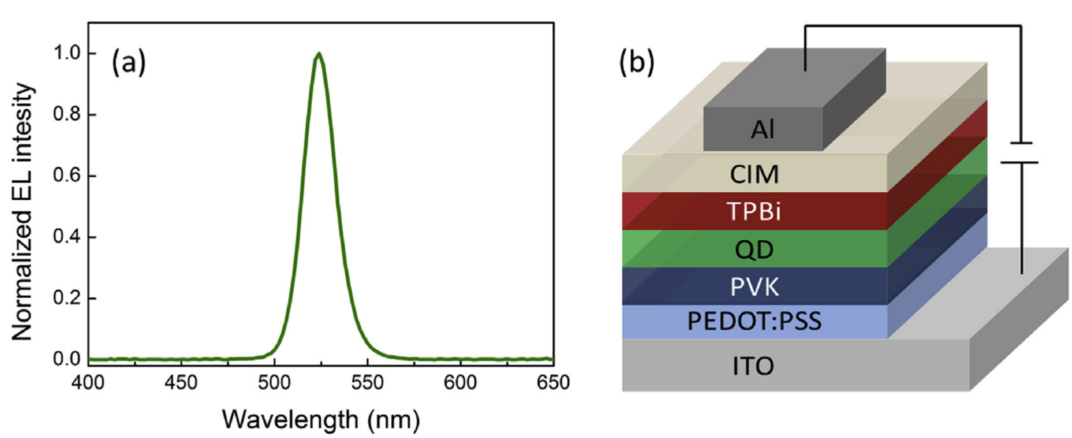

Fig. 1. (a) Normalized electroluminescence (EL) spectrum and (b) the schematic device structure of QLEDs.

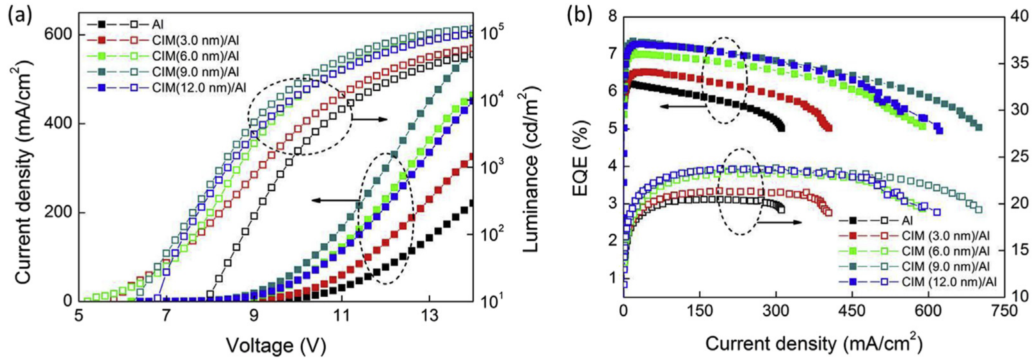

Fig. 2. (a) Current density-voltage-luminance (J-V-L) characteristics for QLEDs with Al-only and CIM/Al cathodes. (b) EQE and CE of these devices as a function of current density.

while the latter gives an EQE of 6.8% and a CE of 21.8 cd/A, as shown in Fig. 3(b). It should be noticed that even in optimized LiF/Al-based QLEDs, charges are not well balanced because the electrons are more easily injected into the QD emissive layer than the holes due to the different energy barriers the carriers encountered [3,4,22]. Such deficiency and corresponding solutions will be discussed in the next paragraphs. Ultraviolet photoelectron spectroscopy (UPS) measurement was applied to explain the role this CIM layer played in QLEDs. Fig. 3(c) shows the secondary-electron cut-off regions of the UPS spectrum of Al film and Phen-NaDPO film on Al, respectively. It can be observed that after depositing Phen-NaDPO onto the Al film, the workfunction (WF) of the system (calculated by the equation WF = 21.2 eV−E_{cutoff}) has been decreased from 3.5 eV to 3.3 eV. To some extent, the reduced WF of cathode in QLED facilitates the electron injection into active layers, therefore improving the device performance [16,20].

Charge balance is an important factor for QLEDs in achieving high performance [4,6–8,11,27]. It has been well recognized that in QLEDs with regular structure (ITO as anode and metal as cathode), electrons are injected spontaneously from the cathode while holes encounter barriers during the injection process because of the deep valance-band energy level of quantum dots, resulting in an unbalanced charge injection [4,8,28,29]. Therefore, it is possible to balance the electron and hole currents by impeding the electron injection from cathode in the working device under forward bias [27]. For this purpose, the Phen-NaDPO was introduced as a buffer layer between the electron transporting layer and LiF-based cathode. As can be clearly observed from Fig. 4 (a), an even higher EQE of 8.5% and peak CE over 29 cd/A are achieved by the combined cathode configuration (Phen-NaDPO/LiF/Al) compared with the performance of LiF-based device, demonstrating the positive effect of this CIM.

In order to confirm that such improved performance is indeed related to the balanced charge injection which should be attributed to the decreased electron current, electron-only (ITO/

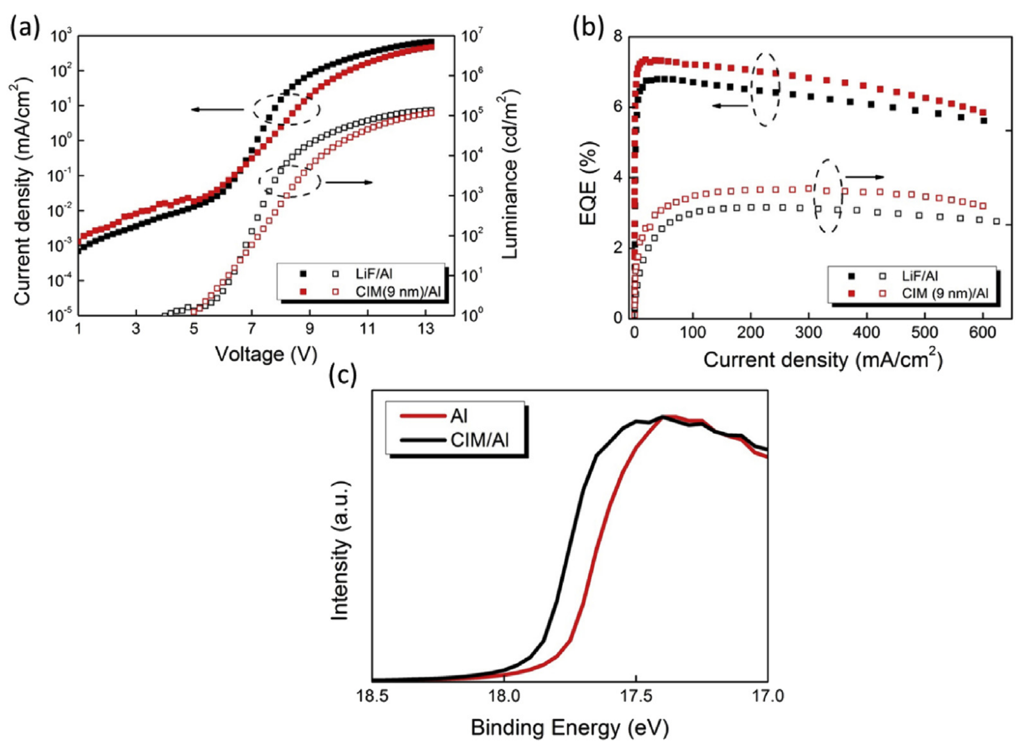

Fig. 3. (a) Current density-voltage-luminance (J-V-L) characteristics of the devices based on QLEDs with LiF/Al and CIM(9 nm)/Al cathodes, respectively. (b) EQE and CE of these two devices as a function of current density. (c) UPS spectra of the secondary-electron cut-off regions for Al and Phen-NaDPO/Al, respectively.

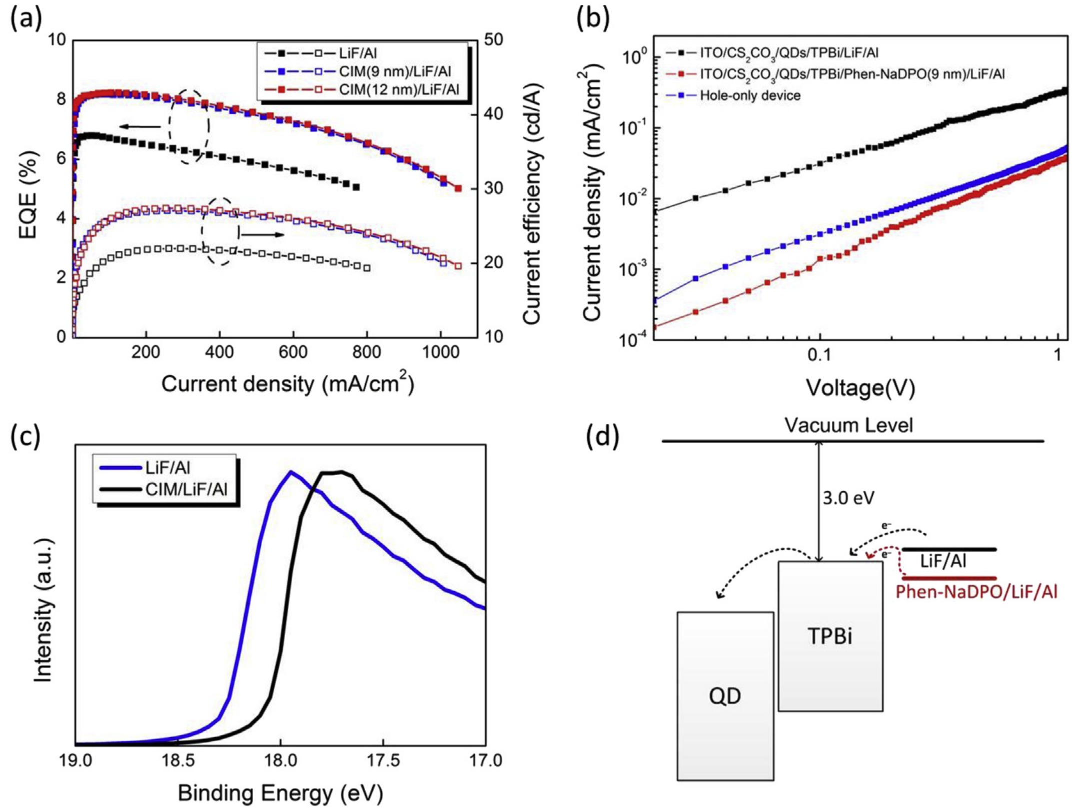

Fig. 4. (a) EQE and CE of the devices as a function of current density. (b) Electrical measurements on the current density-voltage curves for the electron-only and hole only devices. (c) UPS spectra of the secondary electron cut-off regions for LiF/Al and Phen-NaDPO/LiF/Al, respectively and (d) Schematic illustration of electron injections in LiF-based device and Phen-NaDPO/LiF/Al-based device.

Cs_2CO_3(2 nm)/QDs/TPBi/(LiF or Phen-NaDPO/LiF)/Al) and hole-only (ITO/PEDOT:PSS/PVK/QDs/Au(300 nm)) devices are fabricated, respectively, and their current density-voltage characteristics are drawn in Fig. 4(b). It should be mentioned that the thicknesses of all the layers in the above charge-only devices are identical to those used in the working devices. It is clearly reflected that the current density of the electron-only device is more than one order of magnitude greater than that of the hole-only device with a structure of ITO/PEDOT:PSS/PVK/QDs/Au. However, after inserting a 9-nm-thick Phen-NaDPO layer, the current densities for electron-only device are suppressed and, more importantly, closer to the current densities of the hole-only device, which further supports that a better charge balance has been achieved in the working device with the incorporation of Phen-NaDPO. Meanwhile, according to our previous discussion, it is also expected that the WF of such cathode configuration (Phen-NaDPO/LiF/Al) changes because of the existence of Phen-NaDPO. Fig. 4(c) shows the UPS spectra of secondary-electron cut-off regions of LiF/Al and Phen-NaDPO/LiF/Al films, respectively. The calculated WF of LiF/Al is around 2.91 eV while the Phen-NaDPO/LiF/Al gives a value of 3.14 eV. Considering the fact that the lowest unoccupied molecular orbital (LUMO) level of TPBi is around 2.9–3.0 eV [30], the higher WF of the cathode of Phen-NaDPO/LiF/Al (3.14 eV) cathode can block parts of the injected electrons, as illustrated in Fig. 4(d), contributing to an improved charge balance and better device efficiency. Meanwhile, such variations in the WFs are also in good agreement with the decreased current densities of single-carrier devices in the above mentioned discussions (shown in Fig. 4(b)). While hole-transport materials (TCTA, CBP, etc.) [31] or insulator (poly(methyl methacrylate), PMMA) [4] have been utilized to reduce the electron injection for better device performance, Phen-NaDPO acts as the interfacial layer with enhanced electron injection and device performance has been successfully demonstrated in the Phen-NaDPO/Al QLEDs.

4. Conclusion

In conclusion, an organic cathode interfacial material with promising electron transport and a high T_g has been introduced in QLEDs. Better device performance, including the brightness, EQE and CE are simultaneously achieved in our devices compared with the reference devices without a CIM. The CIM-based device even shows a higher EQE and CE compared with LiF-based devices while giving similar J-V characteristics. UPS measurements were utilized to explain the functions of Phen-NaDPO in QLED based on the reduced WF of cathode for better electron injection. Moreover, the combination of Phen-NaDPO and LiF as a bilayer can further improve the device performance with a peak EQE of 8.5% and a CE over 29 cd/A. Incorporating the organic CIM led to a more balanced electron/hole injection from both electrodes and thus enhanced device performance.

Acknowledgments

The work is financially supported by the National Research Foundation of Singapore (NRF-CRP11-2012-01). XHZ is grateful to the financial support of NSFC, MOST, SCUT and Guangdong province (Grant Nos. 2015CB655000, 201101C0105067115, 51173051 and U1301243).

References

[1] V. Colvin, M. Schlamp, A. Alivisatos, Light-emitting diodes made from

cadmium selenide nanocrystals and a semiconducting polymer, Nature 370 (1994) 354–357.
[2] B. Dabbousi, M. Bawendi, O. Onitsuka, M. Rubner, Electroluminescence from CdSe quantum-dot/polymer composites, Appl. Phys. Lett. 66 (1995) 1316–1318.
[3] L. Qian, Y. Zheng, J. Xue, P.H. Holloway, Stable and efficient quantum-dot light-emitting diodes based on solution-processed multilayer structures, Nat. Phot. 5 (2011) 543–548.
[4] X. Dai, Z. Zhang, Y. Jin, Y. Niu, H. Cao, X. Liang, L. Chen, J. Wang, X. Peng, Solution-processed, high-performance light-emitting diodes based on quantum dots, Nature 515 (2014) 96–99.
[5] K.H. Lee, J.H. Lee, H.D. Kang, B. Park, Y. Kwon, H. Ko, C. Lee, J. Lee, H. Yang, Over 40 cd/A efficient green quantum dot electroluminescent device comprising uniquely large-sized quantum dots, ACS Nano 8 (2014) 4893–4901.
[6] Y.X. Yang, Y. Zheng, W.R. Cao, A. Titov, J. Hyvonen, J.R. Manders, J.G. Xue, P.H. Holloway, L. Qian, High-efficiency light-emitting devices based on quantum dots with tailored nanostructures, Nat. Phot. 9 (2015) 259–266.
[7] X.Y. Yang, Y. Ma, E. Mutlugun, Y. Zhao, K.S. Leck, S.T. Tan, H.V. Demir, Q. Zhang, H. Du, X.W. Sun, Stable, efficient, and all-solution-processed quantum dot light-emitting diodes with double-sided metal oxide nanoparticle charge transport layers, ACS Appl. Mater. Interfaces 6 (2013) 495–499.
[8] X.Y. Yang, E. Mutlugun, Y. Zhao, Y. Gao, K.S. Leck, Y. Ma, L. Ke, S.T. Tan, H.V. Demir, X.W. Sun, Solution processed tungsten oxide interfacial layer for efficient hole-injection in quantum dot light-emitting diodes, Small 10 (2014) 247–252.
[9] X.Y. Yang, D.W. Zhao, K.S. Leck, S.T. Tan, Y.X. Tang, J.L. Zhao, H.V. Demir, X.W. Sun, Full visible range covering InP/ZnS nanocrystals with high photometric performance and their application to white quantum dot light-emitting diodes, Adv. Mater. 24 (2012) 4180–4185.
[10] Y. Shirasaki, G.J. Supran, M.G. Bawendi, V. Bulovic, Emergence of colloidal quantum-dot light-emitting technologies, Nat. Phot. 7 (2013) 13–23.
[11] B.S. Mashford, M. Stevenson, Z. Popovic, C. Hamilton, Z.Q. Zhou, C. Breen, J. Steckel, V. Bulovic, M. Bawendi, S. Coe-Sullivan, P.T. Kazlas, High-efficiency quantum-dot light-emitting devices with enhanced charge injection, Nat. Phot. 7 (2013) 407–412.
[12] A. Rizzo, M. Mazzeo, M. Palumbo, G. Lerario, S. D'Amone, R. Cingolani, G. Gigli, Hybrid light-emitting diodes from microcontact-printing double-transfer of colloidal semiconductor CdSe/ZnS quantum dots onto organic layers, Adv. Mater. 20 (2008) 1886–1891.
[13] W.K. Bae, J. Kwak, J.W. Park, K. Char, C. Lee, S. Lee, Highly efficient green-light-emitting diodes based on CdSe@ ZnS quantum dots with a chemical-composition gradient, Adv. Mater. 21 (2009) 1690–1694.
[14] B.N. Pal, Y. Ghosh, S. Brovelli, R. Laocharoensuk, V.I. Klimov, J.A. Hollingsworth, H. Htoon, ‘Giant’CdSe/CdS core/shell nanocrystal quantum dots as efficient electroluminescent materials: strong influence of shell thickness on light-emitting diode performance, Nano Lett. 12 (2011) 331–336.
[15] X.Y. Yang, Y. Divayana, D.W. Zhao, K.S. Leck, F. Lu, S.T. Tan, A.P. Abiyasa, Y.B. Zhao, H.V. Demir, X.W. Sun, A bright cadmium-free, hybrid organic/quantum dot white light-emitting diode, Appl. Phys. Lett. 101 (2012) 233110.
[16] L.S. Hung, C.W. Tang, M.G. Mason, Enhanced electron injection in organic electroluminescence devices using an Al/LiF electrode, Appl. Phys. Lett. 70 (1997) 152–154.
[17] S.E. Shaheen, C.J. Brabec, N.S. Sariciftci, F. Padinger, T. Fromherz, J.C. Hummelen, 2.5% efficient organic plastic solar cells, Appl. Phys. Lett. 78 (2001) 841–843.
[18] K.S. Yook, S.O. Jeon, S.Y. Min, J.Y. Lee, H.J. Yang, T. Noh, S.K. Kang, T.W. Lee, Highly efficient P-I-N and tandem organic light-emitting devices using an air-stable and low-temperature-evaporable metal azide as an n-dopant, Adv. Funct. Mater. 20 (2010) 1797–1802.
[19] H. Liao, L. Chen, Z. Xu, G. Li, Y. Yang, Highly efficient inverted polymer solar cell by low temperature annealing of Cs_2CO_3 interlayer, Appl. Phys. Lett. 92 (2008) 173303.
[20] G. Jabbour, B. Kippelen, N. Armstrong, N. Peyghambarian, Aluminum based cathode structure for enhanced electron injection in electroluminescent organic devices, Appl. Phys. Lett. 73 (1998) 1185–1187.
[21] S. Coe-Sullivan, J.S. Steckel, W.K. Woo, M.G. Bawendi, V. Bulović, Large-area ordered quantum-dot monolayers via phase separation during spin-casting, Adv. Funct. Mater. 15 (2005) 1117–1124.
[22] J.M. Caruge, J.E. Halpert, V. Bulovic, M.G. Bawendi, NiO as an inorganic hole-transporting layer in quantum-dot light-emitting devices, Nano Lett. 6 (2006) 2991–2994.
[23] P. Anikeeva, C. Madigan, J. Halpert, M. Bawendi, V. Bulović, Electronic and excitonic processes in light-emitting devices based on organic materials and colloidal quantum dots, Phys. Rev. B 78 (2008) 085434.
[24] Q. Sun, Y.A. Wang, L.S. Li, D. Wang, T. Zhu, J. Xu, C. Yang, Y. Li, Bright, multi-coloured light-emitting diodes based on quantum dots, Nat. Phot. 1 (2007) 717–722.
[25] Z. Tan, Y. Zhang, C. Xie, H. Su, J. Liu, C. Zhang, N. Dellas, S.E. Mohney, Y. Wang, J. Wang, Near-band-edge electroluminescence from heavy-metal-free colloidal quantum dots, Adv. Mater. 23 (2011) 3553–3558.
[26] W.Y. Tan, R. Wang, M. Li, G. Liu, P. Chen, X.C. Li, S.M. Lu, H.L. Zhu, Q.M. Peng, X.H. Zhu, W. Chen, W.C.H. Choy, F. Li, J.B. Peng, Y. Cao, Lending triarylphosphine oxide to phenanthroline: a facile approach to high-performance organic small-molecule cathode interfacial material for organic photovoltaics utilizing air-stable cathodes, Adv. Funct. Mater. 24 (2014) 6540–6547.
[27] W.K. Bae, Y.S. Park, J. Lim, D. Lee, L.A. Padilha, H. McDaniel, I. Robel, C. Lee, J.M. Pietryga, V.I. Klimov, Controlling the influence of auger recombination on the performance of quantum-dot light-emitting diodes, Nat. Commun. 4 (2013) 1–8.
[28] W.K. Bae, J. Lim, M. Zorn, J. Kwak, Y.-S. Park, D. Lee, S. Lee, K. Char, R. Zentel, C. Lee, Reduced rfficiency roll-off in light-emitting diodes enabled by quantum dot–conducting polymer nanohybrids, J. Mater. Chem. C 2 (2014) 4974–4979.
[29] T. Ding, X.Y. Yang, L. Bai, Y. Zhao, K.E. Fong, N. Wang, H.V. Demir, X.W. Sun, Colloidal quantum-dot LEDs with a Solution-processed copper oxide (CuO) hole injection layer, Org. Electron. 26 (2015) 245–250.
[30] Y. Zhao, L. Zhu, J. Chen, D. Ma, Improving color stability of blue/orange complementary white OLEDs by using single-host double-emissive layer structure: comprehensive experimental investigation into the device working mechanism, Org. Electron. 13 (2012) 1340–1348.
[31] K.S. Leck, Y. Divayana, D.W. Zhao, X.Y. Yang, A.P. Abiyasa, E. Mutlugun, Y. Gao, S. Liu, S.T. Tan, X.W. Sun, H.V. Demir, Quantum dot light-emitting diode with quantum dots inside the hole transporting layers, ACS Appl. Mater. Interfaces 5 (2013) 6535–6540.
[32] G.E. Jabbour, Y. Kawabe, S.E. Shaheen, J.F. Wang, M.M. Morrell, B. Kippelen, N. Peyghambarian, Highly efficient and bright organic electroluminescent devices with an aluminum cathode, Appl. Phys. Lett. 71 (1997) 1762–1764.
[33] S.E. Shaheen, G.E. Jabbour, M.M. Morrell, Y. Kawabe, B. Kippelen, N. Peyghambarian, M.F. Nanor, R., Schlaf, E.A. Mash, N.R. Armstrong, Bright blue organic light-emitting diode with improved color purity using a LiF/Al cathode, Appl. Phys. Lett. 84 (1998) 2324–2327.